An Octane-Fueled Solid Oxide Fuel Cell

Zhongliang Zhan, *et al.*

Science **308**, 844 (2005);
DOI: 10.1126/science.1109213

Science (print ISSN 0036-8075; online ISSN 1095-9203) is published weekly, except the last week in December, by the American Association for the Advancement of Science, 1200 New York Avenue NW, Washington, DC 20005.

hydrous character that was altered by later exposure of the zircons to crustal metamorphic fluids. The temperatures measured by our Ti thermometer provide strong evidence against this possibility: Even with allowances for subunity TiO_2 activity (Fig. 2), they are simply too low for the zircons to have crystallized from dry siliceous melts (*31*). The restricted range of temperatures suggests, furthermore, that a highly reproducible set of circumstances removed melt fertility from rocks under prograde conditions consistent with crustal anatexis throughout the Hadean. Temperatures for zircons >4.2 Ga are sparse, but the present database hints at a slight down-temperature "focusing" of typical magmatic conditions between 4.35 and 4.0 Ga (Fig. 3, inset).

The simplest scenario is melting in an ensemble of crustal environments not unlike that of today under conditions at or close to water saturation. Taken collectively, our zircon crystallization temperatures mimic expectations for "modern-day" igneous zircons, with most pointing to a crustal anatectic origin.

The present results substantiate the existence of wet, minimum melting conditions at 4.35 to 4.0 Ga inferred from mineral inclusion studies and are consistent with the early Hadean hydrosphere hypothesis (*9*, *10*). They strongly suggest, moreover, that within ~100 million years of formation, Earth had settled into a pattern of crust formation, erosion, and sediment recycling similar to that produced during the known era of plate tectonics. The rapid establishment of this cycle implies, further, that the pace of geologic activity in general (driven by rapid mantle convection) was much faster in the Hadean than in more recent times.

References and Notes

1. W. Benz, W. L. Slattery, A. G. W. Cameron, *Icarus* **66**, 515 (1986).
2. K. Righter, M. J. Drake, *Earth Planet. Sci. Lett.* **171**, 383 (1999).
3. R. L. Armstrong, *Philos. Trans. R. Soc. London Ser. A* **301**, 443 (1981).
4. S. J. Mojzsis *et al.*, *Nature* **384**, 55 (1996).
5. S. A. Bowring, I. Williams, *Contrib. Mineral. Petrol.* **134**, 3 (1999).
6. D. O. Froude *et al.*, *Nature* **304**, 616 (1983).
7. W. Compston, R. T. Pidgeon, *Nature* **321**, 766 (1986).
8. Y. Amelin, D. C. Lee, A. N. Halliday, R. T. Pidgeon, *Nature* **399**, 252 (1999).
9. S. J. Mojzsis, T. M. Harrison, R. T. Pidgeon, *Nature* **409**, 178 (2001).
10. S. A. Wilde, J. W. Valley, W. H. Peck, C. M. Graham, *Nature* **409**, 175 (2001).
11. G. Turner, T. M. Harrison, G. Holland, S. J. Mojzsis, J. Gilmour, *Science* **306**, 89 (2004).
12. E. B. Watson, D. A. Wark, J. B. Thomas, in preparation.
13. B. T. Peppard, I. M. Steele, A. M. Davis, P. J. Wallace, A. T. Anderson, *Am. Mineral.* **86**, 1034 (2001).
14. L. Storm, F. S. Spear, *J. Metamorph. Geol.* **23**, 107 (2005).
15. J. Selverstone, G. Morteani, J.-M. Staude, *J. Metamorph. Geol.* **9**, 419 (1991).
16. R. L. Rudnick *et al.*, in *Proc. Seventh International Kimberlite Conference,* Cape Town, South Africa, J. J. Gurney, S. R. Richardson, Eds. (Red Barn, Cape Town, South Africa, 1999), pp. 728–735.
17. S. S. Sorensen, *J. Metamorph. Geol.* **6**, 405 (1988).
18. D. A. Wark, A. T. Anderson, E. B. Watson, *Eos Trans. AGU* (joint assembly program and abstracts, 2004).
19. E. D. Ghent, M. Z. Stout, *Contrib. Mineral. Petrol.* **86**, 248 (1984).
20. F. J. Ryerson, E. B. Watson, *Earth Planet. Sci. Lett.* **86**, 225 (1987).
21. E. B. Watson, T. M. Harrison, *Earth Planet. Sci. Lett.* **64**, 295 (1983).
22. E. B. Watson, *Contrib. Mineral. Petrol.* **70**, 407 (1979).
23. The ion microprobe analyses were performed at Woods Hole Oceanographic Institution using a Cameca ims 3f. A primary (O^-) ion-beam current of 5 nA was used in most cases, which resulted in a spot size of 15 to 20 μm. Four 30-s acquisition intervals at each spot resulted in a minimum detection limit (MDL) of ~0.1 ppm Ti using the relatively low-abundance isotope ^{49}Ti (5.5% of Ti). Titanium-48 (74% abundance) cannot be used for analysis of zircons with the ims 3f because of interfering $^{96}Zr^{2+}$ (2.8% isotopic abundance). For this reason, previously published values for Ti content of zircons (*32*, *33*) may be too high. The 2σ analytical uncertainty obtained with the ims 3f was ±20% and ±6%, respectively, at the 1- and 10-ppm levels (corresponding to temperatures of ~570° and ~740°C). The analytical error increases the ±10° uncertainty in the thermometer itself (Fig. 1) to ±16° at 570°C and ±11° at 740°C.
24. N. Sleep, K. Zahnle, *J. Geophys. Res.* **103**, 28,529 (1998).
25. F. Holtz, A. Becker, M. Freise, W. Johannes, *Contrib. Mineral. Petrol.* **141**, 347 (2001).
26. Calculated Zr saturation temperatures (*21*) for the 19,034 analyses in the OZCHEM National Whole Rock Geochemistry GIS Database (https://www.ga.gov.au/products; includes Australia, Papua New Guinea, Antarctica, Solomon Islands, and New Zealand) between 40 and 80% SiO_2 for which requisite data are available (*21*) yield a median of 780°C, with more than 80% of all calculated temperatures greater than the mean of our Hadean results (i.e., 696°C). If representative of the Hadean crustal average, then it is highly unlikely that the temperature distribution in Fig. 3 could reflect a limitation imposed by the Zr concentration of crustal rocks.
27. C. K. Brooks, *Geochim. Cosmochim. Acta* **33**, 357 (1969).
28. L. R. Wager, G. M. Brown, *Layered Igneous Rocks* (Oliver and Boyd, Edinburgh, 1968).
29. D. Trail, S. J. Mojzsis, T. M. Harrison, *Geochim. Cosmochim. Acta* **68**, A743 (2004).
30. R. Maas, P. D. Kinny, I. S. Williams, D. O. Froude, W. Compston, *Geochim. Cosmochim. Acta* **56**, 1281 (1992).
31. Water is required to depress the solidus to temperatures below ~960°C—the dry solidus of rocks of broadly granitic character (*34*–*36*).
32. E. A. Belousova, W. L. Griffin, S. Y. O'Reilly, N. I. Fisher, *Contrib. Mineral. Petrol.* **143**, 602 (2002).
33. P. W. O. Hoskin, *Geochim. Cosmochim. Acta* **69**, 637 (2005).
34. O. F. Tuttle, N. L. Bowen, *Geol. Soc. Am. Mem.* **74** (1958).
35. W. C. Luth, R. H. Jahns, O. F. Tuttle, *J. Geophys. Res.* **9**, 759 (1964).
36. J. A. Whitney, *J. Geol.* **83**, 1 (1975).
37. C.-T. Lee, R. L. Rudnick, in *Proc. Seventh International Kimberlite Conference,* Cape Town, South Africa, J. J. Gurney, S. R. Richardson, Eds. (Red Barn, Cape Town, South Africa, 1999), pp. 503–521.
38. S. R. Taylor, S. M. McLennan, *The Continental Crust: Its Composition and Evolution* (Blackwell Scientific, Oxford, 1985).
39. G. B. Morgan VI, D. London, R. G. Luedke, *J. Petrol.* **39**, 601 (1998).
40. J. D. Webster, W. A. Duffield, *Am. Mineral.* **76**, 1628 (1991).
41. J. B. Lowenstern, M. A. Clynne, T. B. Bullen, *J. Petrol.* **38**, 1707 (1997).
42. J. D. Webster, R. D. Congdon, P. C. Lyons, *Geochim. Cosmochim. Acta* **59**, 711 (1995).
43. B. Hanson, J. W. Delano, D. J. Lindstrom, *Am. Mineral.* **81**, 1249 (1996).
44. I. N. Bindeman, J. W. Valley, *J. Petrol.* **42**, 1491 (2001).
45. N. W. Dunbar, P. R. Kyle, *Am. Mineral.* **78**, 612 (1993).
46. N. W. Dunbar, R. L. Hervig, *J. Geophys. Res.* **97**, 15129 (1992).
47. N. W. Dunbar, R. L. Hervig, *J. Geophys. Res.* **97**, 15151 (1992).
48. C. L. Harford, R. S. J. Sparks, A. E. Fallick, *J. Petrol.* **44**, 1503 (2003).
49. P. E. Izbekov, J. C. Eichelberger, B. V. Ivanov, *J. Petrol.* **45**, 2325 (2004).
50. P. A. Cawood, E. C. Leitch, *Proc. Ocean Drill. Prog.* **156**, 343 (1997).

51. We thank E. Baxter, R. Rudnick, L. Storm, F. Spear, and D. Wark for providing rock samples and/or zircon separates for the thermometry calibration, and M. Hamilton for the Skaergaard zircons. We also thank G. Layne (ion microprobe), D. Wark, S. Mojzsis, P. Holden, E. Q. Reid, Z. Bruce, S. Mussett, and J. Thomas for scientific discussions and assistance with analytical aspects. The work was supported at Rensselaer Polytechnic Institute by NSF grants EAR 0073752 and EAR 0440228 (to E.B.W.), at Australian National University by Australian Research Council grant DP0342709 (to T.M.H.), and at the University of California, Los Angeles, by grants from the NSF Earth Sciences: Instrumentation and Facilities (EAR/IF) program and NASA's Exobiology program and National Astrobiology Institute.

Supporting Online Material

www.sciencemag.org/cgi/content/full/308/5723/841/DC1
Fig. S1

9 February 2005; accepted 14 March 2005
10.1126/science.1110873

An Octane-Fueled Solid Oxide Fuel Cell

Zhongliang Zhan and Scott A. Barnett*

There are substantial barriers to the introduction of hydrogen fuel cells for transportation, including the high cost of fuel-cell systems, the current lack of a hydrogen infrastructure, and the relatively low fuel efficiency when using hydrogen produced from hydrocarbons. Here, we describe a solid oxide fuel cell that combines a catalyst layer with a conventional anode, allowing internal reforming of *iso*-octane without coking and yielding stable power densities of 0.3 to 0.6 watts per square centimeter. This approach is potentially the basis of a simple low-cost system that can provide substantially higher fuel efficiency by using excess fuel-cell heat for the endothermic reforming reaction.

Improving fuel efficiency is one of the key reasons, along with reduced pollution, for the adoption of fuel cells for applications such as transportation. Improving efficiency not only reduces fuel consumption but also reduces the associated CO_2 emission. Although fuel cells can achieve efficiencies of 50 to 60%, overall "well-to-wheels" efficiencies are cur-

rently only ~29% (*1*) because of the relatively low efficiency of hydrocarbon conversion (i.e., reforming) to H_2, where excess heat must be added. The efficiency may improve to as high as 42% as the technology improves but still may not provide sufficient motivation to replace lower-cost options such as gasoline-electric hybrids with efficiencies of ~32%. Furthermore, H_2 production from hydrocarbons releases as much CO_2 as does direct use in an internal combustion engine, and H_2 is more expensive than gasoline (*2*, *3*). (Hydrogen production from renewable energy sources is not considered here; although this will be a truly pollution-free solution, it will not provide a substantial fraction of global energy needs in the foreseeable future.)

However, there is a well-known method to improve well-to-wheels fuel-cell efficiency to ~50% (*4*) by using excess fuel-cell heat for the endothermic reforming reaction. Solid oxide fuel cells (SOFCs) are well suited for this because their operating temperatures are high enough to provide the high-temperature heat needed for reforming (*5*). There has been considerable recent interest in SOFCs for efficient auxiliary electrical power generation for heavy- and light-duty vehicles, as well as aircraft (*6*, *7*). With reductions in SOFC operating temperature, there may also be interest in battery/SOFC hybrid technology for vehicle propulsion, in which the SOFC would serve as a battery charger with relatively infrequent cycling (frequent on-off cycling would likely be problematic for high-temperature SOFCs). A transportation SOFC would likely use internal reforming within the stack, both because the system is simplified (a separate reformer system is not needed) and because heat transfer is optimal (*8*). Unfortunately, internal reforming of typical transportation fuels, that is, gasoline and diesel, has not been successful because they cause coking on Ni-based SOFC anodes (*9*).

Here, we describe a SOFC design that combines a catalyst layer with a conventional anode that allows internal reforming of *iso*-octane without coking and yields stable power densities of 0.3 to 0.6 W/cm^2. *Iso*-octane, a high-purity compound similar to gasoline, was used in these experiments to achieve a demonstration of the feasibility of SOFCs with transportation fuels. This avoids a number of experimental complications with commercial fuels, which typically contain a number of different compounds and additives with a substantial range of compositions, as well as relatively large amounts of sulfur contaminants that can seriously affect fuel-cell performance. The experiments were done with conventional SOFCs at ~800°C or with low-temperature (<600°C) SOFCs that may be more suitable for transportation applications.

Many of the experiments used SOFCs similar to those being developed worldwide (*10*). These SOFCs consisted of a thin yttria-stabilized zirconia (YSZ) electrolyte layer, a thick Ni-YSZ anode support, and a composite cathode consisting of $La_{0.8}Sr_{0.2}MnO_3$ (LSM) and 8 mol% Y_2O_3-stabilized ZrO_2 (YSZ) or $La_{0.6}Sr_{0.4}Co_{0.2}Fe_{0.8}O_3$ (LSCF) and $Ce_{0.9}Gd_{0.1}O_{1.95}$ (GDC) (*4*). Without any modification, these SOFCs were unstable when used with *iso*-octane/CO_2/H_2O fuel streams. Examples of the decrease in cell voltage for constant current operation at 770°C with three different fuel compositions—6% *iso*-octane/94% CO_2, 3% *iso*-octane/72% CO_2/25% steam, or 5% *iso*-octane/76% CO_2/19% air—are shown in Fig. 1. The degradation was caused by severe coke buildup on the Ni-YSZ anode, which was visible to the eye in many cases. A scanning electron microscope energy-dispersive x-ray spectrum (fig. S2A) (*4*) taken from the SOFC anode after degradation showed a clear carbon peak along with the expected Ni, Zr, and Y peaks.

Two modifications were required to achieve stable operation with *iso*-octane fuel mixtures. First, a porous catalyst layer—an ~0.5-mm-thick piece of stabilized zirconia with a thin layer of Ru-CeO_2 on both sides (total Ru loading 2 mg/cm^2 in all cases)—was placed against the anode side of the SOFC. The effect of the catalyst layer can be seen by comparing curves 1 and 4 in Fig. 1, which were both obtained with 6% *iso*-octane balanced by CO_2. The cell was much more stable with the catalyst than without, showing a nearly constant voltage, although subsequent observation indicated very slight carbon deposition on the catalyst layer. Although the initial cell voltages in curves 1 and 4 are similar, the current density was lower for curve 4 because of the catalyst layer; the lower current was not the reason for the improved stability, however, because SOFC stability against coking generally degrades as current decreases (*11*). Second, the addition of a small amount of air to the fuel yielded fully stable performance (curve 5 in Fig. 1) without measurable carbon deposits detected on the catalyst layer or the fuel cell (as shown in fig. S2B) (*4*).

A differentially pumped mass spectrometer was used to observe the products of the

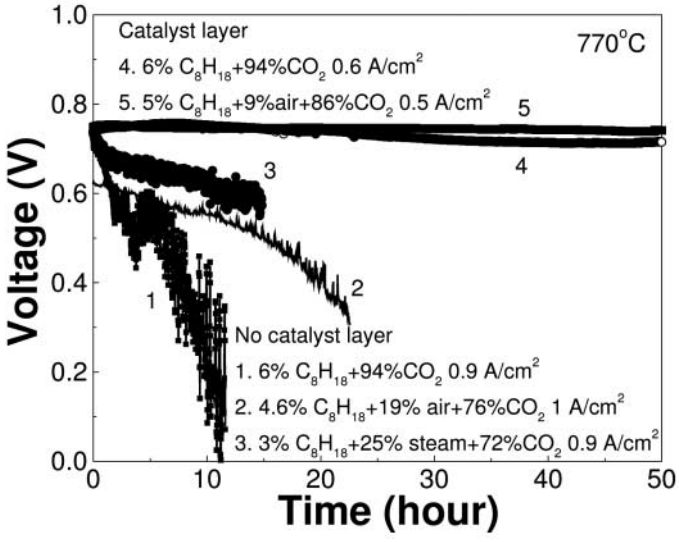

Fig. 1. Life tests of anode-supported SOFCs (Ni-YSZ|YSZ|LSM-YSZ, LSM) operated on various *iso*-octane/CO_2/steam/air mixtures with or without a catalyst layer at 770°C.

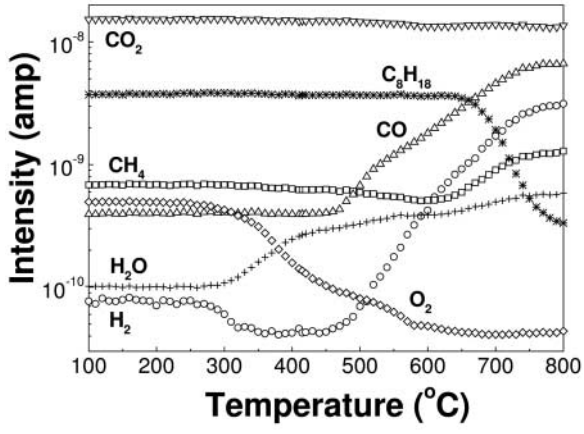

Fig. 2. Mass spectrometer peak intensities versus temperature for 5% *iso*-octane/9% air/86% CO_2 fuel mixtures after flowing over a Ru-CeO_2 catalyst layer at 100 SCCM.

Department of Materials Science and Engineering, Northwestern University, 2220 Campus Drive, Evanston, IL 60208, USA.

*To whom correspondence should be addressed. E-mail: s-barnett@northwestern.edu

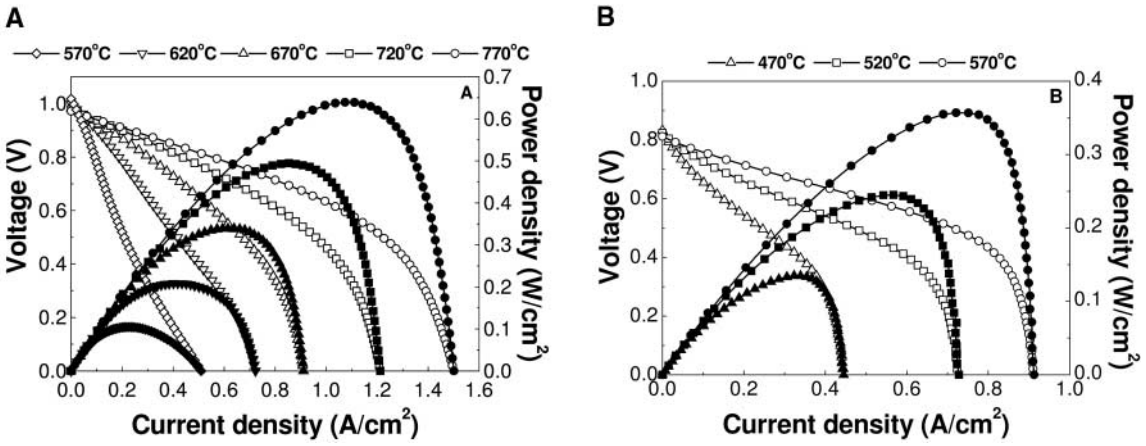

Fig. 3. Voltage and power density versus current density for the cell, tested in 5% *iso*-octane/9% air/86% CO_2 at 100 SCCM in the anode and ambient air in the cathode at different cell temperatures. (**A**) NiO-YSZ|YSZ|LSCF-GDC, LSCF, with a catalyst layer, Ru-CeO_2|PSZ|Ru-CeO_2. (**B**) NiO-SDC|SDC|LSCF-GDC, LSCF, with a catalyst layer, Ru-CeO_2|PSZ-CeO_2|Ru-CeO_2.

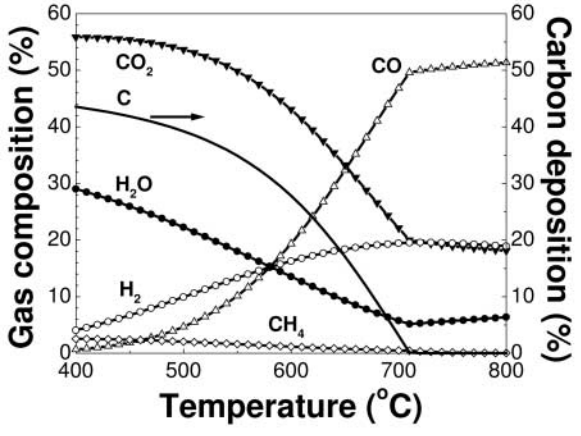

Fig. 4. Calculated equilibrium product distribution as a function of temperature for a 5% *iso*-octane/9% air/86% CO_2 inlet fuel mixture.

fuel reactions on the Ru-CeO_2 catalyst. A description of the measurement and typical mass spectra (fig. S3) are given in (*4*). For a 5% *iso*-octane/9% air/86% CO_2 mixture flowing at 100 standard cubic centimeters per minute (SCCM) over the catalyst, there was no apparent reaction below ~280°C, that is, the H_2, CO, and CH_4 peaks were at background levels whereas CO_2, *iso*-octane, and O_2 did not decrease (Fig. 2). The O_2 peak decreased with increasing temperature from ~280°C to 550°C, which indicates that *iso*-octane oxidation was occurring. No change in the *iso*-octane peak was detected in this range, because the O_2 amount was sufficient to react at most 10% of the *iso*-octane. The primary reaction products that can be used by the SOFC, CO, and H_2 did not begin to increase measurably until the temperature reached ~550°C. This change, along with the corresponding decrease in the *iso*-octane peak that became obvious above ~650°C, indicated that dry reforming was occurring. Above 700°C, a small amount of methane was observed.

Typical stable cell performance at different temperatures in *iso*-C_8H_{18}/CO_2/air with the catalyst layer (Fig. 3A) exhibited open-circuit voltages from 0.97 to 1.02 V that tended to increase with decreasing temperature, which is consistent with the thermodynamically predicted values of 0.99 to 1.03 V. The maximum power densities ranged from 0.1 W/cm² at 570°C to 0.6 W/cm² at 770°C. The cells were stable over a wide range of operating conditions, not just the high currents shown in Fig. 1. For example, cells kept at zero current for 50 hours with 5% *iso*-octane/9% air/86% CO_2 maintained a stable open-circuit voltage without coking on the anode or the catalyst layer (fig. S4) (*4*).

The results in Fig. 3A illustrate a typical trend in YSZ-electrolyte SOFCs: Power densities drop significantly below ~650°C (*12*). Lower temperature SOFCs are desired for transportation applications, so we also tested reduced-temperature SOFCs with thin Sm-doped ceria (SDC) electrolytes, thick Ni-SDC supports, and composite cathodes containing LSCF and GDC. Figure 3B shows an example of SOFC/catalyst performance with *iso*-octane/CO_2/air fuel. The catalyst layer and air addition were found to be important for maintaining stable, coke-free operation over typical 50- to 100-hour tests (figs. S5 and S6) (*4*). The SDC cells yielded maximum power densities of ~0.35 W/cm² at 570°C, a value comparable to those reported for other SDC-electrolyte cells operated on H_2 (*13*). The open-circuit voltage was relatively low for these cells because of the electronic conductivity in SDC electrolytes (*13*). The maximum power values were limited in part by the increase in slope seen in the voltage-current curves at high current (Fig. 3B). Such behavior is often attributed to limited gas transport through one or both electrodes (*14*) and is not surprising given the present thick anodes and low H_2 partial pressures below 600°C (Fig. 2). Thus, increasing the fuel H_2 content by improving the low-temperature catalyst performance is one possible means to improve upon the cell performance in Fig. 3B.

The above results showed that the catalyst layer was crucial for allowing stable cell operation without coking. Based on the thermodynamic analysis shown in Fig. 4, the present fuel compositions were stable against coking at temperatures >720°C but were within the coking regime for the lower temperature cells. Coking can still occur on Ni catalysts even under thermodynamically non-coking conditions (*9*). Recent studies have shown that Ni is especially well suited for growing carbon fibers (*15*). Coking from carbon-containing gases on metal catalysts like Fe or Co has also been observed (*16*). It is nonetheless desirable to use Ni or similar metals in SOFC anodes because they are very good electrochemical catalysts (*17*). Recent studies have used Cu as an anode conductor because it is inert against coking and reforming; unfortunately, it is not a good electrochemical catalyst, such that power densities were typically relatively low (*18*).

The present cells had conventional Ni-based anodes to achieve good power densities and a catalyst layer to prevent coking. The lack of coking at the Ni-based anode can be explained by reforming at the Ru-Ceria catalyst layer, which eliminated most of the hydrocarbon species before the fuel reached the anode. A key element of this strategy was the choice of a catalyst metal, Ru, that promotes hydrocarbon reforming but does not itself cause coking (*19*). For some of the conditions used here (<720°C), coking was expected (Fig. 4), yet no carbon was observed on the

catalyst layer in any case, even for the low-temperature experiments (fig. S6B). The coking on Ru was presumably kinetically limited.

There are three minor drawbacks to the catalyst layer. First, it is expected to reduce the rate at which fuel can diffuse to the anode, thereby decreasing cell power density. Indeed, test results at 770°C typically showed lower power densities of ~0.6 W/cm^2 with the catalyst layer compared with initial values (prior to degradation) of 0.8 to ~1 W/cm^2 without the layer. Second, because the catalyst layer was electrically insulating in the present experiments, electrical current collection could be an issue. However, a slight modification of a typical interconnect design, in which the catalyst layer is present only in the interconnect gas-flow channels as shown schematically in fig. S7 (*4*), could be used to provide good current collection. Third, Ru is expensive, although less so than precious metal catalysts such as Pt and Rh. As discussed in the supplemental materials (*4*), this cost should not be prohibitive for reasonable Ru loadings.

The other factor required for stable cell operation was having at least 10% air in the fuel mixture. This represents a 2% oxygen addition to the fuel, and it is not clear what role this plays in preventing coking. One possibility is that the oxygen helps remove carbon on the catalyst. Although the addition of oxygen amounts to burning some of the fuel, the amount of air is too small to substantially reduce the efficiency or to substantially dilute the fuel with nitrogen.

The present results compare favorably with other recently reported methods for using heavy hydrocarbon fuels in SOFCs. SOFCs have recently been reported to operate successfully on N_2-diluted gasoline (*18*) and other heavy hydrocarbon fuels (*20*). However, the power densities were substantially lower (0.1 W/cm^2) than in the present results. Prototype SOFC systems have recently been developed for vehicle auxiliary electrical power using external partial-oxidation reforming of gasoline to produce a hydrogen-rich fuel (*6*). However, partial-oxidation reforming has substantially lower efficiency than is possible with H_2O-CO_2 reforming (*21*). In cases where reforming is done within the stack but away from the cells (*22*) or in an external reformer (*23*), heat transfer is not as good and additional hardware is required. One disadvantage of direct internal reforming is that the endothermic reaction may be too rapid and may cause substantial SOFC or catalyst cooling near the fuel inlet (*24*). The present catalyst layer may have an advantage in this regard, because the catalyst material can be varied to suitably adjust the rate of the reforming reaction. The addition of oxygen to the fuel also helps mitigate this cooling because of the exothermic partial-oxidation reaction.

The present small-scale demonstrations show the feasibility of SOFCs fueled by hydrocarbons such as *iso*-octane, with substantial advantages including high efficiency, a relatively simple system design, and reduced operating temperature. However, more work needs to be done to prove that this approach is practical with real fuels such as gasoline, diesel, and aircraft fuels; recently developed techniques for reducing sulfur contamination to low levels (*25*) may be especially useful.

References and Notes

1. Toyota Fuel Cell Hybrid Vehicle, www.toyota.co.jp/en/tech/environment/fchv/fchv12.html (2004).
2. United States Council for Automotive Research, Hydrogen as a Fuel; www.uscar.org/Media/2002issue2/hydrogen.htm (2004).
3. U. Bossel, B. Eliasson, G. Taylor, European Fuel Cell Forum, Report E08, 15 April 2003; www.efcf.com/reports.
4. Materials and methods are available as supporting material on *Science* Online.
5. N. Minh, in *Proc. 8th Int. Symp. on Solid Oxide Fuel Cells*, S. C. Singhal, M. Dokiya, Eds. (Electrochemical Society, Pennington, NJ, 2003), p. 43.
6. S. Mukerjee, S. Shaffer, J. Zizelman, in *Proc. 8th Int. Symp. on Solid Oxide Fuel Cells*, S. C. Singhal, M. Dokiya, Eds. (Electrochemical Society, Pennington, NJ, 2003), p. 88.
7. S. C. Singhal, *Solid State Ionics* **152–153**, 405 (2002).
8. J. Rostrup-Nielsen, L. J. Christiansen, *Appl. Catal. Gen.* **126**, 381 (1995).
9. R. J. Gorte, J. M. Vohs, *J. Catal.* **216**, 477 (2003).
10. J. W. Stevenson, in *Proc. 8th Int. Symp. on Solid Oxide Fuel Cells*, S. C. Singhal, M. Dokiya, Eds. (Electrochemical Society, Pennington, NJ, 2003), p. 31.
11. Y. Lin, Z. Zhan, J. Liu, S. A. Barnett, *Solid State Ionics*, in preparation.
12. J. Liu, S. A. Barnett, *J. Am. Ceram. Soc.* **85**, 3096 (2002).
13. C. Xia, F. Chen, M. Liu, *Electrochem. Solid State Lett.* **4**, A52 (2001).
14. Z. Zhan, J. Liu, S. A. Barnett, *Appl. Catal. Gen.* **262**, 255 (2004).
15. M. L. Toebes, J. H. Bitter, A. J. Dillen, K. P. Jong, *Catal. Today* **76**, 33 (2002).
16. N. Rodriguez, *J. Mater. Res.* **8**, 3233 (1993).
17. A. Atkinson *et al.*, *Nat. Mater.* **3**, 17 (2004).
18. R. J. Gorte, H. Kim, J. M. Vohs, *J. Power Sources* **106**, 10 (2002).
19. A. T. Ashcroft, A. K. Cheetham, M. L. H. Green, P. D. F. Vernon, *Nature* **352**, 225 (1991).
20. Z. F. Zhou, C. Gallo, M. B. Pague, H. Schobert, S. N. Lvov, *J. Power Sources* **133**, 181 (2004).
21. J. Botti, in *Proc. 8th Int. Symp. on Solid Oxide Fuel Cells*, S. C. Singhal, M. Dokiya, Eds. (Electrochemical Society, Pennington, NJ, 2003), p. 16.
22. R. A. George, A. C. Casanova, S. E. Veyo, in *2002 Fuel Cell Seminar Abstr.*, Fuel Cell Seminar Committee, Eds. (Courtesy Associates, Washington, DC, 2002), p. 977.
23. J. Devitt, J. Xu, C. Lukaniuk, G. Price, M. Staite, in *Proc. 8th Int. Symp. on Solid Oxide Fuel Cells*, S. C. Singhal, M. Dokiya, Eds. (Electrochemical Society, Pennington, NJ, 2003), p. 1276.
24. K. Ahmed, K. Foger, *Catal. Today* **63**, 479 (2000).
25. R. T. Yang, A. J. Hernandez-Maldonado, F. H. Yang, *Science* **301**, 79 (2003).

Supporting Online Material

www.sciencemag.org/cgi/content/full/1109213/DC1
Materials and Methods
SOM Text
Figs. S1 to S7
References

28 December 2004; accepted 15 March 2005
Published online 31 March 2005;
10.1126/science.1109213
Include this information when citing this paper.

From Dimming to Brightening: Decadal Changes in Solar Radiation at Earth's Surface

Martin Wild,[1]* Hans Gilgen,[1] Andreas Roesch,[1] Atsumu Ohmura,[1] Charles N. Long,[2] Ellsworth G. Dutton,[3] Bruce Forgan,[4] Ain Kallis,[5] Viivi Russak,[6] Anatoly Tsvetkov[7]

Variations in solar radiation incident at Earth's surface profoundly affect the human and terrestrial environment. A decline in solar radiation at land surfaces has become apparent in many observational records up to 1990, a phenomenon known as global dimming. Newly available surface observations from 1990 to the present, primarily from the Northern Hemisphere, show that the dimming did not persist into the 1990s. Instead, a widespread brightening has been observed since the late 1980s. This reversal is reconcilable with changes in cloudiness and atmospheric transmission and may substantially affect surface climate, the hydrological cycle, glaciers, and ecosystems.

Solar radiation at Earth's surface (also known as global radiation or insolation) is the primary energy source for life on our planet. Widespread measurements of this quantity began in the late 1950s. Trends in worldwide distributed observational records of solar radiation have been proposed in various studies (*1–5*). These studies report a general decrease of sunlight over land surfaces on the order of 6 to 9 W m^{-2} from the beginning of the measurements in about 1960 until 1990, corresponding to a decline of 4% to 6% over 30 years. Such a decrease may profoundly influence surface temperature, evaporation, the hydrological cycle, and ecosystems, as noted in (*6–10*).

Thus far, no study has addressed the evolution of solar radiation from 1990 onward, because extensive observational data after 1990 were not easily accessible. The main source for data prior to 1990 in (*1–5*) was the Global Energy Balance Archive (GEBA) (*11*), which